Predicting the Resultant Cutting Force in Hard Turning Using Machine Learning Techniques

Chahrazed Hiba Mimoun
Research Laboratory of Industrial Technologies, Faculty of Applied Sciences, University of Tiaret, Algeria
hiba.mimoun@univ-tiaret.dz

Kamel Haddouche
Research Laboratory of Industrial Technologies, Faculty of Applied Sciences, University of Tiaret, Algeria
haddouchekam@gmail.com (corresponding author)

Souâd Makhfi
Department of Mechanical Engineering, Faculty of Applied Sciences, University of Tiaret, Algeria
msouad71@gmail.com

Received: 27 April 2025 | Revised: 22 June 2025 and 28 June 2025 | Accepted: 8 July 2025

 DOI: https://doi.org/10.48084/etasr.11759

ABSTRACT

In the machining process, the cutting force is used for several purposes, including adaptive control, online tool wear observation, and monitoring. Its modeling and computation are the main facets of metal cutting theory, recognizing that many parameters influence its value. Despite the analytical and numerical approaches developed, the current trend is to use artificial intelligence tools for prediction. In this context, machine-learning techniques are used to predict the resulting cutting force during the hard longitudinal turning of AISI 52100 steel by a cBN insert. This study used Artificial Neural Networks (ANN), Adaptive Neuro-Fuzzy Inference System (ANFIS), Support Vector Machines (SVM), and Gaussian Process Regression (GPR). For each model, the response is the resultant cutting force, with machining conditions such as workpiece hardness, cutting speed, feed, and depth-of-cut as inputs. The predicted results are compared with the experimental data to determine the effectiveness of the predictive models, showing that ANFIS is the most promising, offering the best performance.

Keywords-prediction; force; hard turning; machine learning; AISI 52100; cBN insert

I. INTRODUCTION

Hard turning has supplemented or even replaced conventional grinding, which is often time-consuming and expensive when machining precision parts. This is because it offers the possibility of replacing several consecutive grinding operations with a single one. In addition, hard turning allows for higher material removal rates than grinding, eliminates the need for lubricants, and thus favors dry machining. Knowledge of the thermomechanical loads acting on the tool is required for the estimation of machine-tool power and the design of elements effectively rigid and free of vibrations. Machining force modeling and computation are one of the main problems in metal cutting theory. Different interactive variables that influence cutting force (cutting speed, feed, depth-of-cut, tool geometry and coating, etc.) pose a challenge to develop a mathematical model to achieve the desired performance [1].

This study considered oblique cutting. In this context, the first studies aimed to understand the cutting process based on the Merchant's model. In [3], an orthogonal theory with assumptions was used to predict forces in oblique cutting. The same approach was followed in [4] and [5]. In [6, 7], oblique cutting models with different angles of inclination were proposed. In [8], the impact of the side and back rake angles of the tool on the cutting force was studied. Further investigations considered the radius and chamfer of the tool tip. A summary of the analytical models developed for oblique cutting is documented in [9]. In addition, many numerical approaches used FEM in machining processes to predict characteristics, including cutting forces, cutting temperature, chip morphology, tool wear, surface integrity, residual stresses, etc. [10].

As part of the application of artificial intelligence tools, Machine Learning (ML) is increasingly used to analyze large datasets and predict the performance of processes. In this context, many researchers have attempted to apply ML techniques in machining. This study is a continuation of [11, 12], where ANN, multiple regression, and the Response Surface Method (RSM) were used to predict cutting forces and

residual stresses. Specifically, this study used four ML models, namely ANN, ANFIS, SVM, and GPR, to estimate the resulting cutting force (F_c) when turning an AISI 52100 bearing steel using a cBN cutting tool. Machining conditions such as cutting speed (V_c), feed (f), depth-of-cut (a_p) and workpiece hardness (HRC) are taken as inputs, while F_c is the output. To determine the effectiveness of the predictive models, the results based on prediction are compared with experimental data to determine the best one for predicting the resultant cutting force.

II. MODELING

This section provides the mathematical formulations and building features in the MATLAB environment for each model.

A. ANN Approach

A conventional feedforward ANN based on a three-layer architecture was employed. The first layer represents the inputs, and the last one is the output. The intermediate layer is the hidden one, which contains neurons that perform internal processing. The output s_j of each neuron is given by:

$$s_j = g\left(\sum_{i=1}^{n} w_{ij} \cdot e_i - b_j\right) \quad (1)$$

where e_i denotes the inputs, which represent cutting parameters (V_c, f, a_p) and workpiece hardness (HRC). g is the activation or transfer function of the neuron. The weights w_{ij} and bias b_j are adjustable parameters. In the ANN design under MATLAB, the user can select the transfer function, the number of hidden neurons, and the learning algorithm during compilation to enhance predictions. This study used a linear activation function for the output and a hyperbolic tangent sigmoid one for the single hidden layer. In addition, Bayesian regularization was selected as the training algorithm [11, 12]. The choice of the number of hidden neurons was established after considering various ANN structures 4-x-1 by varying x. From Table I, it can be observed that the better prediction was attained for 4-11-1 and 4-12-1 structures, which give the minimum MSEN (Mean Square Error for Normalized data) and the higher correlation coefficient (R). The final selection between the two structures is discussed in Section IV.

TABLE I. CHOICE OF HIDDEN NEURONS

Structure	Performance indicators		
	R	R2	MSEN
4-8-1	0.98335	0.96697722	0.0081
4-9-1	0.98308	0.96644629	0.0082
4-10-1	0.9833	0.96687889	0.0081
4-11-1	0.98348	0.96723291	0.0080
4-12-1	0.98345	0.9671739	0.0080
4-13-1	0.98332	0.96691822	0.0081
4-14-1	0.98315	0.96658392	0.0082

B. ANFIS Model

The ANFIS architecture consists of a cascade of five layers: fuzzy layer (L_1), product layer (L_2), normalized layer (L_3), defuzzy layer (L_4), and total output layer (L_5). ANFIS combines the strengths of neural networks and fuzzy logic to model complex systems. The following equations provide the ANFIS formulation with two inputs x_1 and x_2:

$$L_{1,i} = \mu A_i(x_1), \quad \text{for } i = 1, 2 \ldots j \quad (2)$$

$$L_{1,i} = \mu B_i(x_2), \quad \text{for } i = 1, 2 \ldots j \quad (3)$$

$$L_{2,i} = W_i = \mu A_i(x_1) \cdot \mu B_i(x_2), \text{ for } i = 1, 2 \ldots j^2 \quad (4)$$

$$L_{3,i} = \overline{W}_i = \frac{W_i}{\sum_{i=1}^{j^2} W_i} \quad (5)$$

$$L_{4,i} = \overline{W}_i f_i = \overline{W}_i (p_i x_1 + q_i x_2 + r_i) \quad (6)$$

$$L_{5,i} = \overline{W}_i f_i \quad (7)$$

with μA_i and μB_i denoting the membership functions and p_i, q_i, and r_i being linear parameters. In this work, ANFIS has four inputs, hence a longer development of equations. Sugeno's FIS, which is commonly documented as appropriate to model the nonlinearities of systems, was considered. Under the toolbox Neuro-Fuzzy Designer of MATLAB, several FIS structures were tested to select the one that gives better predictions. The 8-3-2-2 configuration offered the best performance. In addition, a triangular membership function was selected at the input, and a constant one was applied at the output.

C. SVM Model

The parameters of the SVR comprise the coefficients α_i, support vectors X_i, and bias term b are calculated to formulate the following regression function:

$$f(x) = \sum \alpha_i K(X_i, x) + b \quad (8)$$

with K being the kernel function. In the toolbox regression learner of MATLAB, SVM models can be based on six distinct kernel functions: linear, quadratic, cubic, fine-Gaussian, medium-Gaussian, and coarse-Gaussian.

D. GPR Model

Given a training dataset with input x_i and target y_i values, the relationship between them is as follows:

$$y_i = f(x_i) + \zeta_i \quad (9)$$

where ζ_i is an additive Gaussian noise with a mean of zero. In a Gaussian Process (GP), the observed target variable is represented by:

$$x_i \approx GP(m(x_i), k(X, X')) \quad (10)$$

where $m(x_i)$ is the mean function and $k(X, X')$ is the covariance matrix. Four covariance functions are available in the toolbox regression learner of MATLAB: rational quadratic, squared exponential, Matern 5/2, and exponential.

For the SVM and GPR models, the selection of kernel and covariance functions is mentioned in Section IV.

III. EXPERIMENTAL DATA

The machining process considered is a dry longitudinal hard turning of AISI 52100 steel with a cBN 35° diamond type insert. The experimental protocol is documented in [13]. The cutting condition values between min and max are as follows:

- Hardness of work-material (HRC): 45-55.25 HRC.
- Cutting speed (V_c): 50-300 m/min.

- Feed (f): 0.05 ÷ 0.2 mm/rev.
- Depth-of-cut (a_p): 0.1-0.4 mm.

The cutting parameters (V_c, f, a_p) are the operational quantities chosen by the machine-tool operator, while hardness characterizes the material being machined. Notice that the work material is elaborated in [13], and the experiment is focused on determining the influence of the microstructure and cutting parameters on the material behavior of bearing steel AISI 52100 in hard turning. In oblique turning, the interaction between the cutting tool and workpiece produces three orthogonal components of the machining force: feed force (F_f), radial force (F_r), and tangential cutting force (F_t) [11]. A piezoelectric dynamometer type Kistler 9257B acquired these components. The resultant cutting force (F_c) is calculated by:

$$F_c = \sqrt{F_f^2 + F_r^2 + F_t^2} \quad (11)$$

TABLE II. TRAINING DATASET

Test no.	Cutting conditions				
	HRC	V_c (m/min)	f (mm/rev)	a_p (mm)	*Obs.* F_c (N)
1	45	100	0.1	0.2	172.64
2	45	150	0.05	0.2	73.93
3	45	150	0.1	0.2	112.19
4	45	150	0.1	0.3	189.14
5	45	150	0.15	0.2	182.76
6	45	200	0.1	0.2	124.59
7	50	100	0.1	0.2	159.03
8	50	150	0.05	0.2	128.66
9	50	150	0.1	0.4	254.87
10	50	150	0.2	0.2	262.87
11	50	200	0.1	0.1	139.94
12	51.5	50	0.1	0.2	161.86
13	51.5	150	0.1	0.2	146.08
14	51.5	250	0.1	0.2	140.22
15	51.5	300	0.1	0.4	185.08
16	54	100	0.1	0.2	132.85
17	54	150	0.05	0.2	83.78
18	54	150	0.1	0.3	183.48
19	54	150	0.15	0.2	173.52
20	54	150	0.2	0.2	216.60
21	54	200	0.1	0.2	134.30
22	55.25	50	0.1	0.2	192.63
23	55.25	150	0.1	0.2	117.83
24	55.25	200	0.1	0.2	86.08
25	55.25	300	0.1	0.2	137.54

TABLE III. TESTING DATASET

Test no.	Cutting conditions				
	HRC	V_c (m/min)	f (mm/rev)	a_p (mm)	*Obs.* F_c (N)
26	45	150	0.08	0.2	105.62
27	45	150	0.12	0.1	88.60
28	50	150	0.1	0.3	220.17
29	50	150	0.15	0.2	200.78
30	51.5	50	0.1	0.4	190.60
31	51.5	300	0.1	0.2	132.65
32	54	150	0.1	0.2	134.18
33	54	150	0.1	0.4	238.38
34	55.25	100	0.1	0.2	129.71
35	55.25	250	0.1	0.2	125.53

The predictive models are based on a learning process, where the experimental dataset, with 35 tests, is segregated into two subsets: training (70%) and testing (30%) [11, 12]. DoE has already been elaborated in [11]. Tables II and III describe the training and testing data, respectively.

IV. SIMULATION RESULTS

This section presents the simulation results for the four predictive models (ANN, ANFIS, SVM, and GPR). To obtain better predictions, the data were normalized for the ANN and ANFIS approaches. The simulations were carried out in the MATLAB 2023b environment.

A. Training Phase of the ANN

Two ANN structures, 4-11-1 and 4-12-1, were used, which presented close performance in training. In testing, the 4-12-1 ANN achieved better performance and was finally selected. Figure 1 shows the fitted regression between the observed and predicted values in the training phase for the 4-12-1 ANN.

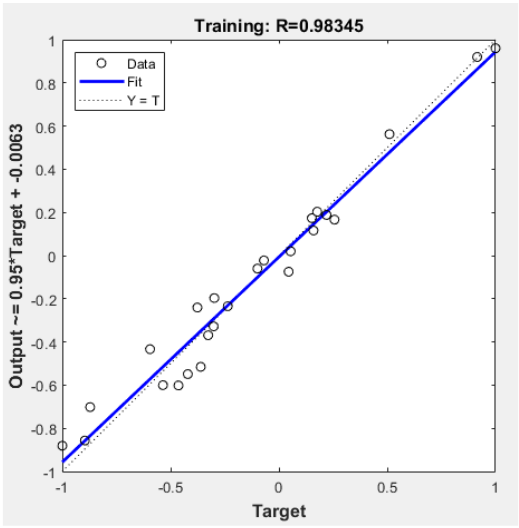

Fig. 1. Fitted regression for ANN in training phase.

B. ANFIS Training

The ANFIS model was trained for 30 epochs considering a grid-partition and hybrid-optimization method that combines least squares and backpropagation. Figure 2 shows that the learning data and the predicted values of the ANFIS are strongly correlated.

C. SVM and GPR learning

For both SVM and GPR techniques, the regression learner toolbox was used in MATLAB, and the resubstitution validation was chosen. For SVM, the model hyperparameters were: Box-constraint "auto mode", Epsilon "auto mode", Kernel-scale "manual = 2", Standardize "yes". In addition, for the GPR model, the hyperparameters were: Basis-function "constant", Use isotropic kernel "yes", Kernel-scale "auto", Sigma-mode "yes", Standardize "yes", Optimize-numeric-parameters "yes". As mentioned in Section II, different kernel and covariance functions can be used. After the simulation of

all cases, the medium-Gaussian kernel function and exponential covariance function gave the best predictions. Figures 3 and 4 show the correlation between the observed and the predicted values of F_c.

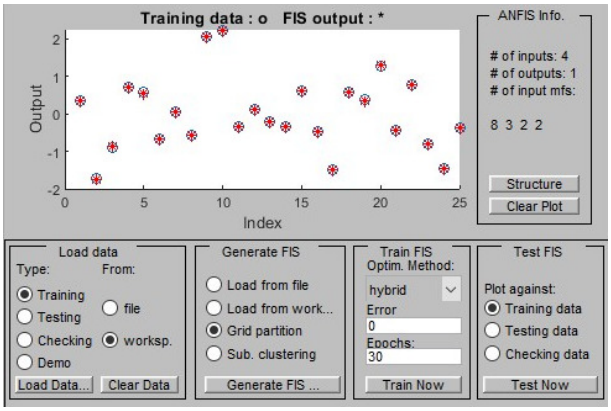

Fig. 2. Training phase of ANFIS.

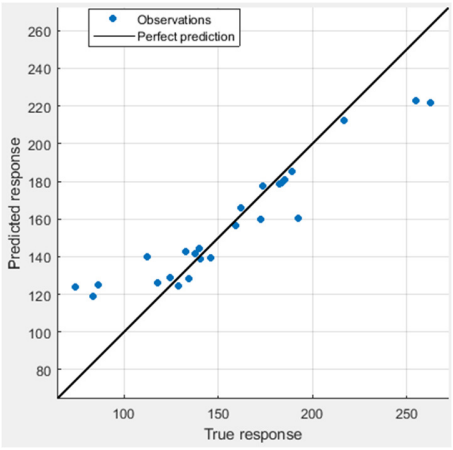

Fig. 3. SVM learning with medium-Gaussian kernel function.

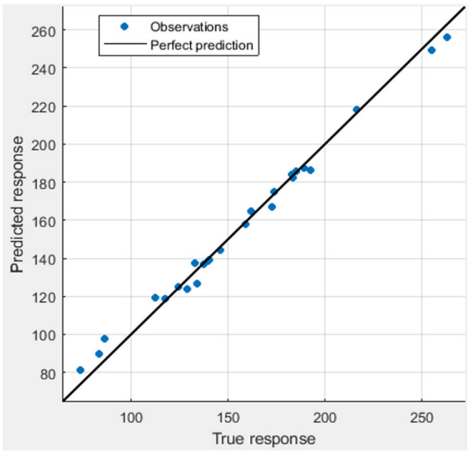

Fig. 4. GPR training with exponential covariance function.

The ANN, SVM, and GPR models show a linear correlation between the observed and the predicted values of F_c in the training phase (Figures 1, 3, and 4). Learning was suitably completed using ANN and GPR, but SVM presented a deviation for a few tests. The best predictor was not selected based only on the learning performance, but on overall performance related to the training and testing phases. This explains why the structure 4-12-1 for the ANN and the medium-Gaussian for SVM were selected.

V. COMPARATIVE ANALYSIS OF THE PREDICTIVE MODELS

R^2, RMSE, and MAPE were used to evaluate the performance of the predictive models between the predicted and observed values:

$$R^2 = 1 - \frac{\sum_{k=1}^{n}\left(F_{c\,obs}(k) - F_{c\,pre}(k)\right)^2}{\sum_{k=1}^{n}\left(F_{c\,obs}(k) - \overline{F_c}_{obs}(k)\right)^2} \quad (12)$$

$$RMSE = \sqrt{\frac{\sum_{k=1}^{n}\left(F_{c\,obs}(k) - F_{c\,pre}(k)\right)^2}{n}} \quad (13)$$

$$MAPE = \frac{100}{n}\sum_{k=1}^{n}\frac{\left|F_{c\,obs}(k) - F_{c\,pre}(k)\right|}{F_{c\,obs}(k)} \quad (14)$$

Table IV summarizes the performance comparison of the models. These results demonstrate that R^2 varies from 0.7784 to 0.9819, the RMSE is between 6.36 and 22.22, and the MAPE ranges from 2.61% to 12.62%. Compared to previous results [11], ML techniques are promising, especially ANFIS. Figures 5 and 6 show, for each test, a comparison between observed and predicted values of the resulting cutting force in the training and testing phases, respectively. As shown in Figure 5, all ML models correlate well in the learning phase, expect SVM. Figure 6 shows that the ANN and ANFIS models demonstrate better performance in the tests.

TABLE IV. PERFORMANCE INDICATORS OF THE PREDICTIVE MODELS

Phase	Indicator and ML model				
	Indicator	**ANN**	**ANFIS**	**SVM**	**GPR**
Training	R^2	0.9669	0.9967	0.8084	0.9898
	RMSE	8.47	2.66	20.35	4.70
	MAPE (%)	5.48	1.15	11.44	2.89
Testing	R^2	0.9249	0.9480	0.7093	0.7196
	RMSE	13.38	11.12	26.32	25.85
	MAPE (%)	5.96	6.24	15.56	14.18
Total	R^2	0.9541	0.9819	0.7784	0.9073
	RMSE	10.12	6.36	22.22	14.37
	MAPE (%)	6.48	2.61	12.62	6.11

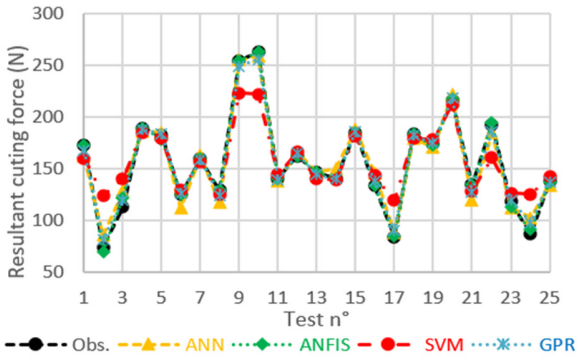

Fig. 5. Comparison of the ML models in their training phases.

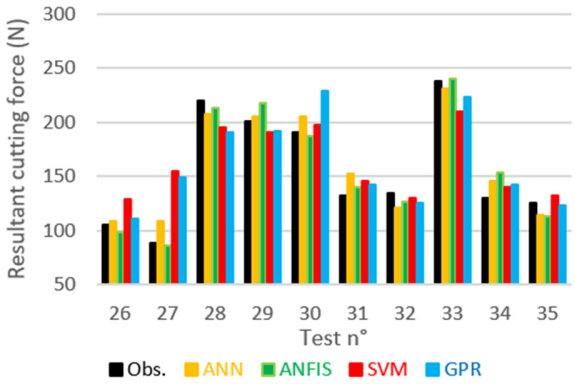

Fig. 6. Comparison of the ML models in their testing stages.

Table V reports the observed and the predicted values of F_c. Figure 7 also shows that all ML models, except SVM, demonstrate satisfactory performance.

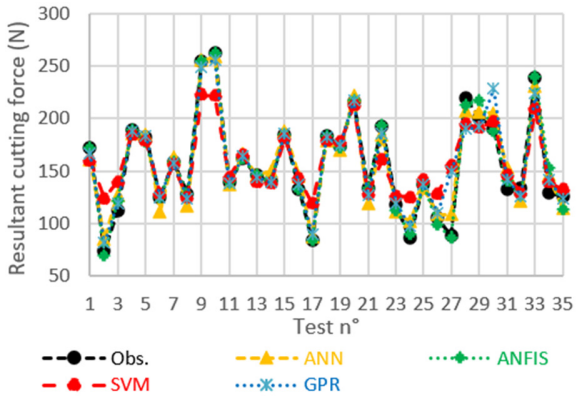

Fig. 7. Comparison of the ML models for the total dataset.

VI. CONCLUSION

This study applied ML techniques for predicting the resultant cutting force during dry longitudinal hard turning of AISI 52100 steel with a cBN insert. A comparative study was conducted, comparing the performance of ANN, ANFIS, SVM, and GPR models on an experimental dataset. The predictive models consider as inputs the workpiece hardness and cutting parameters (cutting speed, feed, and depth-of-cut).

TABLE V. OBSERVED AND PREDICTED VALUES OF F_c

Test no	Observed and predicted values of F_c (N)				
	Obs. F_c	ANN	ANFIS	SVM	GPR
1	172.64	161.33	172.64	160.04	167.15
2	73.93	85.20	69.09	123.87	81.46
3	112.19	127.43	121.49	139.79	119.07
4	189.14	186.19	189.14	185.01	187.65
5	182.76	184.76	178.30	178.61	183.74
6	124.59	111.58	124.59	128.75	125.22
7	159.03	162.71	159.03	156.40	158.01
8	128.66	116.55	128.66	124.49	123.60
9	254.87	255.33	254.87	222.84	249.41
10	262.87	259.16	262.87	221.79	255.92
11	139.94	137.43	139.94	144.10	138.30
12	161.86	166.29	161.86	166.01	164.46
13	146.08	146.23	146.08	139.48	144.17
14	140.22	149.83	140.22	138.86	139.42
15	185.08	187.59	185.08	180.94	185.91
16	132.85	145.68	132.85	142.93	137.49
17	83.78	87.48	84.09	118.70	89.63
18	183.48	179.37	183.48	179.29	182.31
19	173.52	170.28	172.61	177.72	174.65
20	216.60	221.55	217.21	212.38	217.95
21	134.30	119.72	134.30	128.33	126.89
22	192.63	184.14	194.00	160.49	186.24
23	117.83	111.71	112.82	126.14	118.98
24	86.08	102.11	90.37	125.09	97.78
25	137.54	133.55	136.89	141.70	137.04
26	105.62	108.53	98.72	128.67	110.70
27	88.60	108.64	86.52	155.12	149.61
28	220.17	207.81	213.18	194.95	190.29
29	200.78	205.92	217.91	191.12	192.19
30	190.60	205.44	187.54	197.36	228.53
31	132.65	152.67	140.32	146.15	141.99
32	134.18	121.72	126.56	129.92	126.11
33	238.38	230.96	240.40	209.35	223.68
34	129.71	145.76	153.62	140.05	142.14
35	125.53	114.94	113.63	132.25	123.54

- In the learning phase, ANFIS and GPR established higher accuracy ($R^2 \approx 1.0$) with minimum RMSE and MAPE.
- In the testing stage, ANFIS continued to give better predictions, and ANN also showed good performance.

ML techniques were validated against experimental values, indicating their applicability in predicting the resulting cutting force during the hard turning process. ANFIS and ANN appear consistent, achieving better performance. In conclusion, ML techniques, particularly ANFIS, show better ability to predict the resultant cutting force (R^2=0.9819, RMSE=6.36, MAPE=2.61%), indicating a promising approach for enhancing machining processes such as adaptive control.

ACKNOWLEDGMENT

This study was undertaken by a research project in the Laboratory of Industrial Technologies of the University of Tiaret, Algeria, supported by the Directorate-General for Scientific Research and Technological Development (DGRSDT).

REFERENCES

[1] N. A. Fountas, I. Ntziantzias, J. Kechagias, A. Koutsomichalis, J. P. Davim, and N. M. Vaxevanidis, "Prediction of Cutting Forces during Turning PA66 GF-30 Glass Fiber Reinforced Polyamide by Soft Computing Techniques," *Materials Science Forum*, vol. 766, pp. 37–58, 2013, https://doi.org/10.4028/www.scientific.net/MSF.766.37.

[2] G. V. Stabler, "The Fundamental Geometry of Cutting Tools," *Proceedings of the Institution of Mechanical Engineers*, vol. 165, no. 1, pp. 14–26, Jun. 1951, https://doi.org/10.1243/PIME_PROC_1951_165_008_02.

[3] P. L. B. Oxley, "Modelling machining processes with a view to their optimization and to the adaptive control of metal cutting machine tools," *Robotics and Computer-Integrated Manufacturing*, vol. 4, no. 1, pp. 103–119, Jan. 1988, https://doi.org/10.1016/0736-5845(88)90065-8.

[4] G. C. I. Lin, P. Mathew, P. L. B. Oxley, and A. R. Watson, "Predicting Cutting Forces for Oblique Machining Conditions," *Proceedings of the Institution of Mechanical Engineers*, vol. 196, no. 1, pp. 141–148, Jun. 1982, https://doi.org/10.1243/PIME_PROC_1982_196_015_02.

[5] J. A. Arsecularatne, P. Mathew, and P. L. B. Oxley, "Prediction of Chip Flow Direction and Cutting Forces in Oblique Machining with Nose Radius Tools," *Proceedings of the Institution of Mechanical Engineers, Part B: Journal of Engineering Manufacture*, vol. 209, no. 4, pp. 305–315, Aug. 1995, https://doi.org/10.1243/PIME_PROC_1995_209_087_02.

[6] A. Moufki, A. Devillez, D. Dudzinski, and A. Molinari, "Thermomechanical modelling of oblique cutting and experimental validation," *International Journal of Machine Tools and Manufacture*, vol. 44, no. 9, pp. 971–989, Jul. 2004, https://doi.org/10.1016/j.ijmachtools.2004.01.018.

[7] G. Song, S. Sui, and L. Tang, "Precision prediction of cutting force in oblique cutting operation," *The International Journal of Advanced Manufacturing Technology*, vol. 81, no. 1, pp. 553–562, Oct. 2015, https://doi.org/10.1007/s00170-015-7206-z.

[8] S. A. HamaSur and R. M. Abdalrahman, "The Effect of Tool's Rake Angles and Infeed in Turning Polyamide 66," *Engineering, Technology & Applied Science Research*, vol. 13, no. 4, pp. 11204–11209, Aug. 2023, https://doi.org/10.48084/etasr.5891.

[9] M. Storchak and M. A. Lekveishvili, "Improvement of Analytical Model for Oblique Cutting—Part I: Identification of Mechanical Characteristics of Machined Material," *Metals*, vol. 13, no. 10, Oct. 2023, Art. no. 1750, https://doi.org/10.3390/met13101750.

[10] M. Sadeghifar, R. Sedaghati, W. Jomaa, and V. Songmene, "A comprehensive review of finite element modeling of orthogonal machining process: chip formation and surface integrity predictions," *The International Journal of Advanced Manufacturing Technology*, vol. 96, no. 9, pp. 3747–3791, Jun. 2018, https://doi.org/10.1007/s00170-018-1759-6.

[11] S. Makhfi, K. Haddouche, A. Bourdim, and M. Habak, "Modeling of Machining Force in Hard Turning Process," *Mechanics*, vol. 24, no. 3, pp. 367–375, Jun. 2018, https://doi.org/10.5755/j01.mech.24.3.19146.

[12] C. H. Mimoun, K. Haddouche, and S. Makhfi, "A Comparative Study of Multiple Regression, ANN and Response Surface Method for Machining Force," in *Proc. of the Interdisciplinary Conference on Mechanics, Computers and Electrics (ICMECE 2022)*, Barcelona, Spain, 2022, pp. 6–7.

[13] M. Habak, "A study of the influence of the microstructure and cutting parameters on the material behaviour of bearing steel 100Cr6 in hard turning," Ph.D. dissertation, ENSAM, Paris, France, 2006.